

Short Notes

Statistical Significance of the Seismic Coupling Coefficient

by Robert McCaffrey

Abstract Variations in the seismic coupling coefficient (χ), the ratio of the observed to expected seismic moment release rates, at subduction zones are commonly used to make inferences about the physics of subduction. Taking into account the power-law form of the earthquake frequency–moment relation, it is shown that the observed distribution of χ at the world's subduction zones based on the twentieth century's earthquakes can be matched by a single value of $\chi \approx 0.3$ if, as is likely the case, the 90-yr observation time is less than or comparable to the repeat time of the largest possible earthquake. It is shown that because our reliable earthquake record is short, global variations in χ , based on seismicity alone, are poorly resolved and cannot be used to distinguish among subduction models.

Introduction

The theory of plate tectonics has, among other things, allowed us to make predictions about the long-term rate of seismic moment release on faults. Early studies utilizing this predictive capacity found that over time some faults generate roughly the correct amount of seismic moment in earthquakes, but others do not (Brune, 1968; Davies and Brune, 1971). Peterson and Seno (1984) calculated the ratios of the observed to the expected moment rates for most of the world's subduction zones and interpreted these ratios as measures of the coupling on the thrust fault. They went on to relate the variations in this moment ratio to other subduction parameters in order to gain insight into the physics of subduction. Scholz (1990) renamed this ratio the seismic coupling coefficient χ , and Pacheco *et al.* (1993) recalculated values of it for the world's subduction zones using the recently revised catalog of Pacheco and Sykes (1992), which includes earthquakes of $M_w \geq 7$ in this century. Scholz and Campos (1995) amended χ for some of the world's subduction zones by including large earthquakes from the nineteenth century and interpreted variations in it as support for their slab anchor model of subduction.

Brune (1968), whose purpose was to estimate seismic slip rates and not χ , recognized that accurate estimates required a long seismic history due to the random nature of earthquake occurrence. Most other workers who worked with such data also recognized the inherent dangers in making generalizations regarding the long-term seismic behavior of a fault based on the short record. Nevertheless, global variations in χ continue to be used to make inferences about the physics of subduction. The purpose of this article is to test the randomness of our observed χ values that are based on, at best 90 yr and at worst 30 yr, of reliable earthquake moments. It is found that the range of observed χ values

could be generated by subduction zones all with the same actual χ and seismicity distributions. Only the smallest values ($\chi < 0.1$), which are difficult to get at random from a large value of χ , may indicate fundamentally different behavior. However, it is possible to get the full range of observed χ from a small actual χ if the observation time is less than about the repeat time of the largest earthquake. Because such repeat times are likely hundreds of years, today's χ variations probably do not provide useful constraints on the relative merits of subduction models.

Method and Data

We start with the distribution of earthquake moments of the form $N(M_0) = \alpha M_0^{-\beta}$, where N is the number of earthquakes with a seismic moment greater than or equal to M_0 , and α and β are constants that depend on the frequency–magnitude and moment–magnitude relationships (Wyss, 1973; Richter, 1958). β is related to the more common b -value, which is the slope of the log (frequency)–magnitude relationship, by $\beta = 2b/3$. M_0 and M_w will be used interchangeably, noting the relation $M_w = 2/3 \log M_0 - 6.0$, where M_0 is in Newton-meters (Hanks and Kanamori, 1979). Based on earthquake self-similarity, β should equal $2/3$ for earthquakes whose slip dimensions are unbounded by the edges of the fault surface and 1 for the larger events whose slip is limited in one dimension (Rundle, 1989). From the global earthquake catalog of 1900 to 1990, Pacheco *et al.* (1992) estimated that $\beta \approx 0.60$ for $7.0 \leq M_w \leq 7.5$ and $\beta \approx 0.87$ for $7.5 \leq M_w \leq 8.8$, generally in agreement with Rundle's prediction (Pacheco *et al.* actually estimated b). They found that earthquakes of $M_w > 8.8$ are more frequent than predicted by their b -values, which they attributed to

insufficient sampling of the past 90 yr for the truly great earthquakes (their data are plotted in Fig. 1a). However, the disagreement of the $M_w > 8.8$ earthquakes that have slip areas of 100 km or more, with the predictions of self-similarity, may alternatively be due to breakdown of one of the self-similarity assumptions, that is, that the earthquakes do not interact in space or time (Rundle, 1989). In this case, β for $M_w > 8.8$ may not be the same as that observed for the range $7.5 \leq M_w \leq 8.8$.

β controls the ratio of the moment of the largest event to the total moment (Fig. 1b). As β increases, more of the total moment is contained in the smaller, more frequent events. Hence, larger β should result in a more reliable estimate of χ at any given time. At most of the world's subduction zones, the ratio of the largest earthquake moment (in the twentieth century) to total moment is about 20% to 40% (Peterson and Seno, 1984), suggesting that β is between 0.6 and 0.8 (Fig. 1). In the tests, we use the $N(M_w)$ distributions shown in Figure 1a, some of which are observed, some theoretical, some use a single β , and others use separate β for small and large earthquakes.

To determine α , we say that in time T there will be only one earthquake of moment M_0^{\max} or larger, so that $N(M_0^{\max}) = 1$, or $\alpha = (M_0^{\max})^\beta$. T is the "cycle time" defined by Rundle (1989) as the time span during which each earthquake in the distribution has a probability of $1/T$. For the sake of the computation, we specify a lower bound on the earthquakes considered (M_0^{\min}) such that all earthquakes with moments less than it contribute less than 1% to the total seismic moment. Finally, we say that the one earthquake of moment M_0^{\max} or larger has a moment of exactly M_0^{\max} (its minimum possible value) because any larger moment will increase the ratio of the largest to total moment, leading to poorer resolution of χ . In other words, by choosing the minimum moment for this largest earthquake within the bounds $M_0^{\max} \leq M_0 \leq \infty$, we maximize the resolution of χ . The number of earthquakes within a range of moments, say from $M_0 - \Delta M_0$ to $M_0 + \Delta M_0$, is then

$$n(M_0) = N(M_0 - \Delta M_0) - N(M_0 + \Delta M_0) \quad (1)$$

when $M_0^{\min} \leq M_0 \leq M_0^{\max} - \Delta M_0$,

$$n(M_0) = 1 \text{ when } M_0 = M_0^{\max},$$

$$n(M_0) = 0 \text{ when } M_0 < M_0^{\min} \text{ or } M_0 > M_0^{\max}.$$

(The steps ΔM_0 are actually taken as steps of 0.15 in the exponent of the moment to get steps of 0.1 in the magnitude.) From the definition of T , each of the sizes of earthquakes has a probability of occurring in proportion to the number expected; that is, the probability of an earthquake M_0 occurring within a time interval $1/k$ is

$$P(M_0) = n(M_0)/kT, \quad (2)$$

where T is in years and k is the number of time intervals per year. Accordingly, β and M_0^{\max} define a probability density

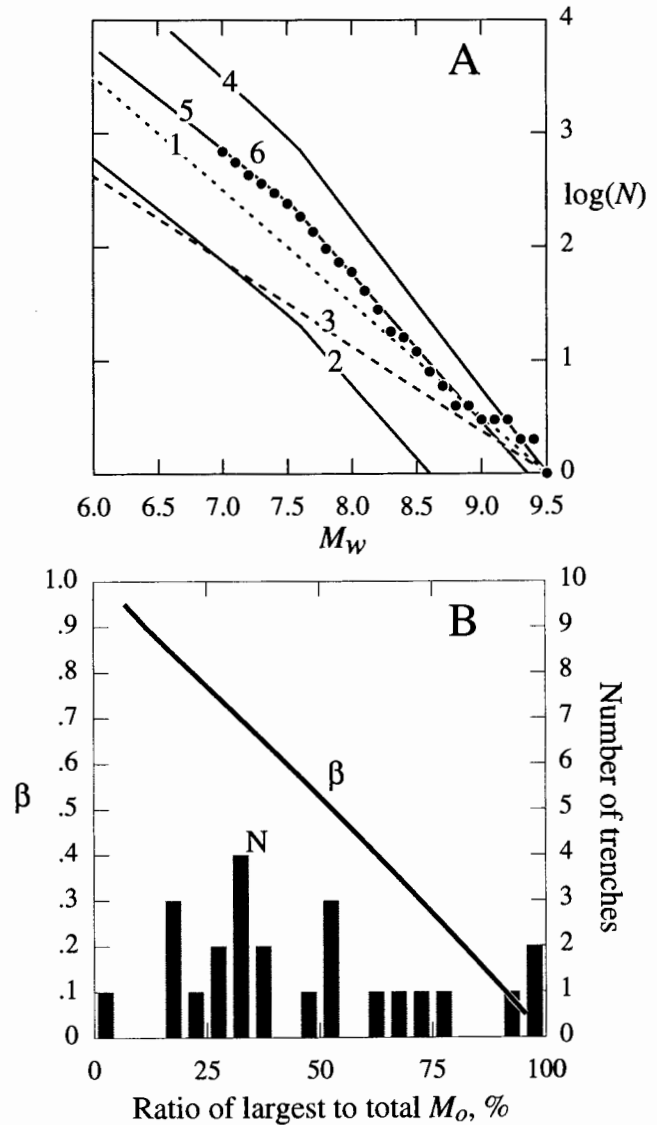


Figure 1. (a) Numbers of earthquakes $N(M_w)$ greater than M_w as a function of M_w for the test cases presented here. Numbers on lines refer to distributions used in test cases shown in Figure 2 as follows: (1) $M_w^{\max} = 9.5$, $b = 1$ (Figs. 2a and 2b); (2) $M_w^{\max} = 8.6$, $b = 0.9$ for $M_w \leq 7.5$, $b = 1.3$ for $7.5 \leq M_w \leq 8.6$ (Fig. 2c); (3) $M_w^{\max} = 9.5$, $b = 0.75$ (Fig. 2d); (4) $M_w^{\max} = 9.5$, $b = 1.0$ for $M_w \leq 7.5$, $b = 1.5$ for $7.5 \leq M_w \leq 9.5$ (Fig. 2e); (5) $M_w^{\max} = 9.35$, $b = 0.9$ for $M_w \leq 7.5$, $b = 1.3$ for $7.5 \leq M_w \leq 9.35$ (Figs. 2f through 2j); and (6 dots) $M_w^{\max} = 9.5$, $N(M_w)$ is observed distribution (1900 to 1990) in the range $7.0 \leq M_w \leq 9.5$ and $b = 1$ for $M_w < 7.0$, from Pacheco *et al.* (1992). Moment is plotted here in terms of M_w instead of M_0 , so the slopes are $-b$ instead of $-\beta$ ($\beta = 2b/3$). (b) Solid line shows the ratio (in percent) of the seismic moment of the largest earthquake to the total moment, as a function of β . Histogram shows the distribution of these percentages at subduction zones, taken from Peterson and Seno (1984). The median is around 35%, corresponding to a β of around 0.6 to 0.8.

function as a function of moment for the earthquakes during time T . For example, if $\beta = 2/3$ and $M_w^{\max} = 9.5$, the total number of expected events of $9.5 \geq M_w \geq 5.0$ is 31,623. If $T = 200$ yr and $k = 365$ (days), then the probability of an earthquake of $9.5 \geq M_w \geq 5.0$ occurring on any particular day is $31,623/73,000$. By definition, one earthquake of M_w^{\max} occurs in time T , so its probability is $1/T$. The total expected moment in time T is $M_e = \sum M_0 n(M_0)$ (summation from M_0^{\min} to M_0^{\max}), and the expected moment rate is then M_e/T .

The procedure used to calculate the seismic coupling coefficient at time t (in years) is to sample the probability density function (2) once during each time step from time 0 to time kt . Because the probability of an earthquake of M_0 occurring in the time period 0 to kt is $kt n(M_0)/kT$, the time step used does not matter in practice as long as the number of time steps in T is greater than the number of earthquakes in T . Each time step will either have an earthquake of $9.5 \geq M_w \geq 5.0$ or no earthquake depending on a random sample of the probability density function. The summed seismic moment for all events that occur up to time t is M_0^E . The apparent seismic coupling coefficient at time t is then

$$\chi(t) = \chi_0 M_0^E / (t M_e / T), \quad (3)$$

where χ_0 is the test value of χ , which can range from 0 to 1, and the denominator is the expected moment in the time 0 to t . The random sampling procedure is run 1000 times each for a duration of $2T$ ($K = 365$) for various combinations of β , χ_0 , T , and M_0^{\max} . For each trial, χ is calculated at $t = T/6$, $T/3$, $T/2$, T , $3T/2$, and $2T$ and plotted as frequency distributions (Fig. 2).

Before presenting the results, a discussion of the meaning of T is warranted because the distributions of χ depend on t/T (3). Also, because our observed values of χ are based on seismicity of the twentieth century only, we must estimate what fraction of T this 90-yr sample represents. The term "recurrence time" commonly refers to the time between the large earthquakes on a fault, and these are often those larger than about magnitude 8. If the largest expected earthquake in time T is a 9.5, then there should also be several earthquakes of $M_w \geq 8$ (Fig. 1a). Hence, T is not the recurrence time, as popularly used in the sense of being the interval between $M_w \geq 8$ earthquakes. The Nankai Trough has had about 12 earthquakes of $M_w \geq 8$ since 684 A.D. (Scholz, 1990), which would suggest that T is more than 2000 yr if the largest earthquake there is a 9.5. However, the largest known earthquakes at the Nankai Trough are about $M_w = 8.6$ (in 1498 and 887 A.D.). Using $M_w^{\max} = 8.6$ and $\beta = 0.87$ predicts six earthquakes of $M_w \geq 8$ during the time T (Fig. 1a). Taking the magnitudes at face value, two earthquakes of the maximum size 8.6 and 12 of $M_w \geq 8$ indicates that two complete cycles have elapsed since 684 A.D. Hence, T for the Nankai Trough is probably close to 650 yr, and the twentieth century is represented by $T/7$. For most

subduction zones, we probably do not have a long enough record to evaluate T , and trying to assign M_0^{\max} for a trench based on the twentieth century's seismicity involves circular reasoning because it assumes that the biggest one has occurred. Nevertheless, we will see that T would have to be as short as a few decades for the 90-yr record to provide reliable estimates of χ .

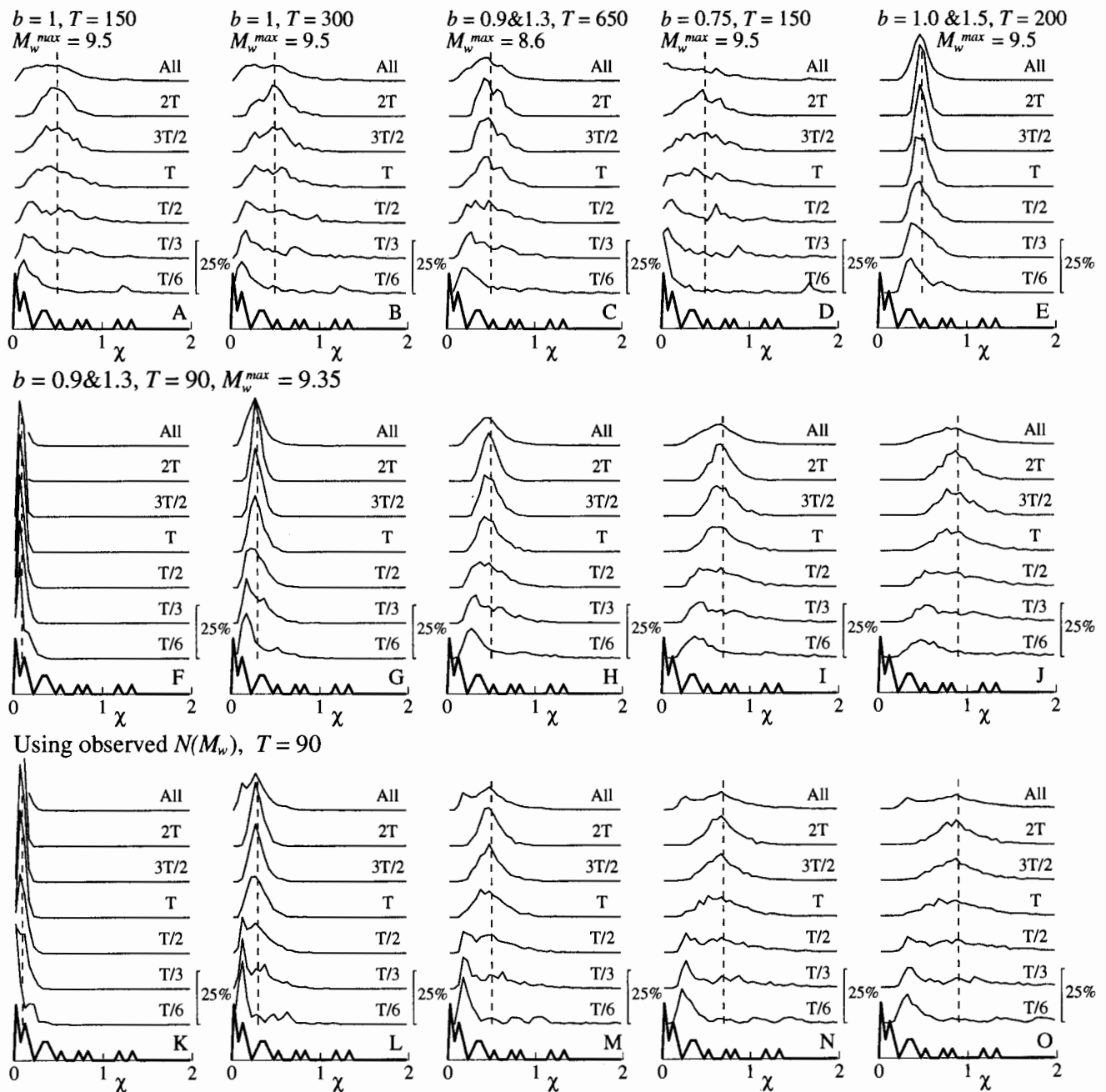
Using earthquake statistics for the 90-yr record, we can estimate a minimum global value of T . A global value of $M_w^{\max} = 9.5$ is used because the 1960 Chile earthquake is the largest reliably known to us in recorded history. However, observed frequency-magnitude relationship for $7.5 \leq M_w \leq 8.8$ earthquakes in the twentieth century predict a single event of $M_w = 9.3$ and not 9.5 (Pacheco *et al.*, 1992) (dashed line in Fig. 1a). Their straight line of $\log [N(M_w)]$ versus M_w can be shifted to intersect $N = 1$ at $M_w = 9.5$ by multiplying N by 2, suggesting that globally, for $M_w^{\max} = 9.5$, $T \approx 180$ yr, or at present, $t = T/2$. For most of the test cases, I use $M_0^{\max} = 2 \times 10^{23}$ N-m ($M_w^{\max} = 9.5$), but it is shown, and self-similarity predicts, that χ does not depend on the M_0^{\max} used.

The calculated distributions of χ will be compared to the distribution of observed values for 23 of the world's subduction zones (Pacheco *et al.*, 1993). These χ 's are based on 90 yr of data from the catalog of Pacheco and Sykes (1992), and I do not take into consideration the uncertainties in them. Nor do I not consider the amendments of Scholz and Campos (1995), who included earthquakes from the nineteenth century at some subduction zones, because the nineteenth century earthquakes cause heterogeneity in the data set, because the uncertainty in moments for them must be at least an order of magnitude, and because the revised χ are too few to impact my conclusions.

Results and Discussion

Figure 2 shows calculated distributions of χ at six times for each of several combinations of T , b , χ_0 , and M_w^{\max} . The top distribution in each panel is the average of the lower six and can be thought to represent the distribution of χ at a fixed time from several subduction zones that have different values of T . The calculated distributions overall show poor resolution of χ at small t . Not only are the variances large, but in most cases, the most probable values (the peaks) are quite different from the true values (shown by dashed lines). Only when t gets to be a large fraction of, or larger than, T does the calculated distribution have its peak at χ_0 . Even at $t = 2T$, the distributions are quite broad compared to the useful range of χ , which is between 0 and 1.

What is not evident from Figure 2 is that at any time the mean of χ is in fact equal to χ_0 . This is expected because the outcome at each time step is independent of all other time steps. The number of independent samples at any time t is the number of trials N_T times the number of time steps kt , where k is the number of time steps per year. In terms of the average calculated χ , this is the same as using kt trials



and N_T time steps. However, the normalized distributions of χ (Fig. 2) depend on kt but not on N_T (unless N_T is too small). For the Earth, the number of trials is 23 (the number of subduction zones), and the average χ for them is 0.3. In tests using $N_T = 23$ and $t = 90$, the average calculated χ is within 0.05 of the trial χ_0 , suggesting that the global average of $\chi \approx 0.3$ may be robust.

The calculated distributions are compared to the 90-yr observed distribution of χ (at bottom, in thicker lines, in Fig. 2) taken from Pacheco *et al.* (1993). The similarity of Figures 2a and 2b shows that the results depend much more on the elapsed time normalized by T than on T itself. The choice of M_w^{\max} has no influence on the χ distributions (compare Figs. 2c to 2h) because it merely shifts the earthquake probability density function along the magnitude axis and does not impact the relative probabilities of any pair of magnitudes below M_w^{\max} .

The relative probabilities of the earthquake magnitudes, determined by b , is the major influence on χ . Increasing b has the effect of increasing the numbers of small earthquakes relative to the big ones, which results in more rapid development of a peak around the correct value of χ (compare Fig. 2a to 2d). Small b produces fewer small events relative to the large ones, resulting in a very peaked distribution (but peaks are not at the correct value; Fig. 2d) because the large, infrequent earthquakes dominate.

The lower values of χ_0 appear to be better resolved than the high values (χ_0 varies across the bottom two rows of Fig. 2) because both the mean and standard deviation of the calculated χ depend directly on χ_0 . For low values of t , the peaks in the estimated values of χ do not correspond with χ_0 . Note that for $\chi_0 = 0.9$, the true value is not evident until $t = T$ (Figs. 2j and 2o).

Figure 2 (middle row) shows tests using $N(M_w)$ distributions taken from the twentieth century's earthquakes. With the constant $\chi_0 = 0.3$ (Fig. 2g), a distribution similar to the observed one is produced when $t \leq T/2$. In Figures 2k through 2o, the observed magnitude distribution (dots in Fig. 1a) is used for $N(M_w)$ in the range $7.0 \leq M_w \leq 9.5$ and $b = 0.9$ for $M_w \leq 7.0$. Again, for the low values of χ_0 and t , the observed distribution of χ is matched quite well (Figs. 2l and 2m).

The point of this report, and shown by Figure 2, is that any particular value of χ_0 can give rise to a large range of apparent values for χ , especially at times that are short compared to T . Moreover, the observed global distribution of χ at subduction zones is matched by some of these randomly generated distributions. The observed distribution is best

matched at $t = T/6$ or $t = T/3$. As suggested above, $T \approx 180$ yr for the whole Earth, but for individual subduction zones, it is probably hundreds of years. If so, then estimates of the variations in χ at subduction zones are not usefully constrained.

The inability in theory to estimate χ will only be compounded by the consideration of uncertainties in the χ estimates themselves, due largely to uncertainties in seismic moments for great and old earthquakes. About all we can say with confidence is that subduction zones without any known history of significant earthquakes probably have a low seismic coupling coefficient. However, we cannot say that subduction zones with known significant earthquakes have a large coupling coefficient. In summary, at present, we cannot rule out that most or all subduction zones have a moderate seismic coupling coefficient of around 0.3.

References

- Brune, J. N. (1968). Seismic moment, seismicity, and rate of slip along major fault zones, *J. Geophys. Res.* **73**, 777–784.
- Davies, G. F. and J. N. Brune (1971). Regional and global fault slip rates from seismicity, *Nature* **229**, 101–107.
- Hanks, T. C. and H. Kanamori (1979). A moment magnitude scale, *J. Geophys. Res.* **84**, 2348–2350.
- Pacheco, J. F. and L. R. Sykes (1992). Seismic moment catalog of large shallow earthquakes, 1900 to 1989, *Bull. Seism. Soc. Am.* **82**, 1306–1349.
- Pacheco, J. F., C. H. Scholz, and L. R. Sykes (1992). Changes in frequency-size relationship from small to large earthquakes, *Nature* **355**, 71–73.
- Pacheco, J. F., L. R. Sykes, and C. H. Scholz (1993). Nature of seismic coupling along simple plate boundaries of the subduction type, *J. Geophys. Res.* **98**, 14133–14159.
- Peterson, E. T. and T. Seno (1984). Factors affecting seismic moment release rates in subduction zones, *J. Geophys. Res.* **89**, 10233–10248.
- Richter, C. F. (1958). *Elementary Seismology*, W. H. Freeman and Co., San Francisco, 1–768.
- Rundle, J. B. (1989). Derivation of the complete Gutenberg-Richter magnitude-frequency relation using the principle of scale invariance, *J. Geophys. Res.* **94**, 12337–12342.
- Scholz, C. H. (1990). *The Mechanics of Earthquakes and Faulting*, Cambridge University Press, New York, 1–439.
- Scholz, C. H. and J. Campos (1995). On the mechanism of seismic decoupling and backarc spreading at subduction zones, *J. Geophys. Res.* **100**, 22103–22115.
- Wyss, M. (1973). Toward a physical understanding of the earthquake frequency distribution, *Geophys. J. R. Astr. Soc.* **31**, 341–360.

Department of Earth and Environmental Sciences
Rensselaer Polytechnic Institute
Troy, New York 12180-3590

Manuscript received 4 November 1996.